

Received July 11, 2021, accepted August 10, 2021, date of publication August 24, 2021, date of current version August 31, 2021.

Digital Object Identifier 10.1109/ACCESS.2021.3106953

A Full-Scale Experimental Investigation on Ride Comfort and Rolling Motion of High-Speed Train Equipped With MR Dampers

S. M. SAJJADI ALEHASHEM^{1,2}, Y. Q. NI^{1,2}, AND X. Z. LIU³

¹Hong Kong Branch of Chinese National Rail Transit Electrification and Automation Engineering Technology Research Center (CNERC-Rail), Hong Kong

²Department of Civil and Environmental Engineering, The Hong Kong Polytechnic University, Hong Kong

³College of Urban Transportation and Logistics, Shenzhen Technology University, Shenzhen 518118, China

Corresponding author: Y. Q. Ni (ceyqni@polyu.edu.hk)

This work was supported in part by the Research Grants Council of Hong Kong Special Administrative Region (SAR) under Grant R-5020-18, in part by the National Natural Science Foundation of China under Grant U1934209, in part by the Wuyi University's Hong Kong and Macao Joint Research and Development Fund under Grant 2019W GALH15 and Grant 2019W GALH17, and in part by the Innovation and Technology Commission of Hong Kong SAR Government under Grant K-BBY1.

ABSTRACT Achieving higher operation speeds safely and comfortably is yet a significant challenge in the railway industry. The rail irregularities and wheel-rail interactions in a train running at high speeds may result in large-amplitude vibration in the train's car body and affect passengers by reducing ride comfort. The train suspension systems have a crucial role in reducing the vibration and improving ride comfort to an acceptable level. In this context, an exclusive semi-active magneto-rheological (MR) damper with a favorable dynamic range was designed and fabricated. The MR dampers were installed in a high-speed train's secondary lateral suspension system in replacement of original passive hydraulic dampers, with intent to mitigate vibration of the car body and keep the ride comfort in a proper level at low and high running speeds. A unique full-scale experimental investigation on the high-speed train equipped with MR dampers was carried out to evaluate the MR damper functionality in a real operating situation. The full-scale roller experiments were conducted in a vast range of speeds from 80 to 350 km/hr. At each speed, different currents were applied to the MR dampers. The car body dynamic responses were collected to evaluate the ride quality of the train. Ride comfort indices under various train operating conditions are calculated through Sperling and UIC513 rules. This study reveals that the designed MR dampers effectively reduce the car body's rolling motion. According to Sperling ride comfort index, the car body vibration was "clearly noticeable" at some running speeds when adopting the MR dampers, but it was not unpleasant. Besides, a "very good comfort" was achieved according to the UIC513 criterion. Also, no train instability was whatsoever observed at high speeds. This experimental investigation bears out the capability of the devised MR damper to achieve desirable ride comfort under high running speeds.

INDEX TERMS High-speed train, MR damper, full-scale experiment, ride comfort index, secondary suspension system.

I. INTRODUCTION

In general, the suspension systems used in railway vehicles are categorized as passive, active, and semi-active [1]. The passive suspension systems commonly used in railway vehicles employing springs and pneumatic or oil dampers have some advantages such as design simplicity and

cost-effectiveness. However, the performance under a wide frequency range of excitations induced by the rail track irregularities is limited, especially at high speeds [2]. The active suspensions have been considered for railway vehicles to improve ride quality and running stability; however, they have limitations in real applications [3]–[7]. The advantages of the semi-active approach compared with the full-active approach are that a separate power supply for the actuator is not necessary, and the required energy is much lower than

The associate editor coordinating the review of this manuscript and approving it for publication was Yingxiang Liu¹.

an active system. Besides, semi-active systems are fail-safe, and in the absence of energy sources, can operate as a passive system.

As far as semi-active dampers are considered, it has been found that MR damper is quite promising for vibration control applications [8]. Some efforts have been taken to illustrate the feasibility and effectiveness of the controlled MR dampers on railway vehicle suspension systems [9]–[13]. MR fluids, which are used in MR dampers, are amongst controllable fluids that respond to applied magnetic fields with dramatic changes in rheological behaviors. The essential feature of the MR fluids is its ability for reversible change from free-flowing viscous liquid to semi-solid with controllable yield strength in milliseconds when exposed to a magnetic field. Compared with conventional semi-active devices such as variable orifice dampers, MR dampers have advantages that they are fast responding, low power requirement, and no moving parts that make them reliable. More detailed descriptions about MR dampers can be found in the literature [14]–[17].

The vibration felt by passengers in a train is caused by the rail irregularities, aroused by contact between the train's wheels and rail. The induced vibration characteristics strongly relate to the train running speed [18]. At a certain running speed, especially at higher speed levels, some vehicle components become extremely unstable due to resonance, and this can result in train instability. To reduce the vibration level and enhance stability, MR damper has been considered to be mounted in the train secondary suspension system [19], [20]. Unlike passive dampers, the dynamic properties of MR dampers are alterable by adjusting the current input to them. Such adjustments affect the dynamic response of the vehicle and the interaction between adjacent compartments of the vehicle, which are coupled together by a series of springs and dampers. For instance, the lateral and yaw motions of the car body coupled with rolling motion can be attenuated through MR dampers installed in the train secondary suspension system in the lateral direction, between the car body and the bogies. However, it may negatively affect ride comfort. So, it is essential to evaluate MR damper's influence on the passenger's ride comfort. Different methods have been developed for evaluating ride comfort of trains under various track and running conditions [21]. Each method has certain advantages and disadvantages, depending on the running condition [22], [23]. Among them, Sperling and UIC513 methods were widely used in the literature. The Sperling index quantifies train ride comfort in both lateral and vertical directions [24], while UIC513 is related to measuring accelerations in all three directions, i.e., longitudinal, lateral, and vertical [30]. In this study, both Sperling and UIC513 methods will be employed to evaluate the ride comfort.

On the other hand, motion sickness is characterized by an unpleasant combination of symptoms, including pallor, sweating, nausea, and vomiting [25] and, consequently, reduces the ride quality. Rolling motion has often been assumed to be a cause of motion sickness, either alone or in combination with motions in other axes [26]. It hypothesizes

that sickness caused by rolling oscillation would depend on the frequency of roll. The frequency dependence of motion sickness produced by rolling oscillation differs from that associated with vertical and horizontal oscillation [26]. The discomfort caused by lateral oscillation with frequencies less than about 0.5 Hz can be reduced by appropriate rolling oscillations. However, with frequencies higher than about 0.5 Hz, roll-compensation increases the discomfort caused by lateral oscillation [27].

Recently, the simulations and numerical studies show a promising potential of MR dampers to be utilized in the train suspension systems. Nevertheless, it needs to be verified through experimental studies before being widely applied to the railway industry. Up to now, a few experimental investigations have been conducted to explore the effectiveness of MR dampers on a full-scale train in running conditions [28], [29]. As a pioneering study, Ni *et al.* [28] experimentally assessed the effectiveness of two types of MR dampers for attenuating vibration of a high-speed train car body. In their study, two different kinds of MR dampers were designed and manufactured. The type-A MR dampers function like a stiffness component, rather than an energy-dissipative device, while the type-B MR dampers exhibit significant damping proportional to the current input. The first stage results revealed favorable dynamic properties and working ranges of the MR dampers, with some valuable suggestions on devising more appropriate MR dampers achieved. In this study, as a succession of the first stage study, an exclusive MR damper with a wider force range and lower friction force was designed and manufactured. The new MR dampers were installed in the train secondary suspension system in the lateral direction, replacing the original passive hydraulic dampers. The train equipped with MR dampers ran on a roller test rig under various speeds from 80 km/h to 350 km/h, in which the track irregularities measured from an in-service high-speed railway were applied as excitations. In the meantime, the MR dampers were tuned simultaneously at different current inputs (from 0 A to 2.0 A). Altogether, 48 train operating conditions were tested with the corresponding car body dynamic behaviors measured with accelerometers and displacement sensors. Both ride comfort and rolling motion of the carriage were evaluated. The main objective of this study is to investigate the efficiency of the devised MR damper through a full-scale dynamic test at different running speeds in conjunction with the evaluation of the carriage ride comfort when being equipped with the MR damper. This investigation pushes forward the feasibility of using semi-active MR suspension system in high-speed trains, enabling their operation in a safer and more comfortable manner.

II. PREPARATION OF EXPERIMENT

A unique, comprehensive full-scale roller test was conducted on a high-speed train equipped with the devised MR dampers to evaluate the ride quality and rolling motion of the train car body. The tested unit is a traction carriage of a Chinese

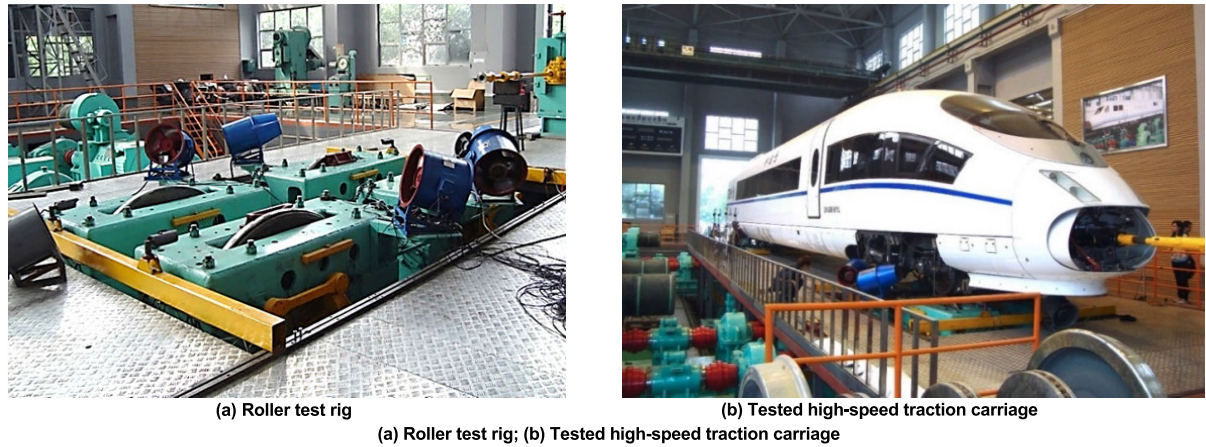


FIGURE 1. Test setup.

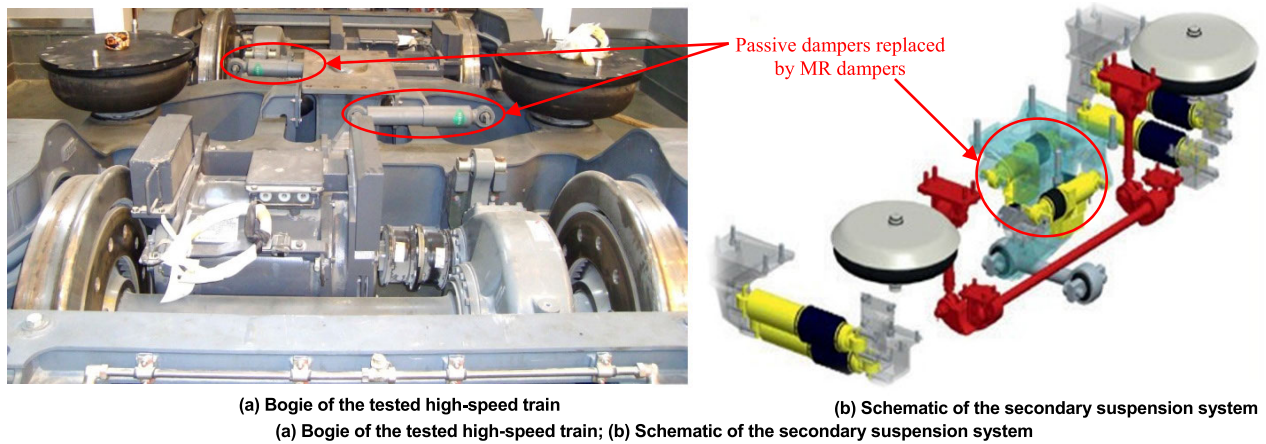


FIGURE 2. Details of the high-speed train bogie.

TABLE 1. Dynamic parameters of the tested car body.

Parameter	Value
Axle load	160 kN
Radius of wheels	0.4575 m
Wheel mass	1,400 kg
Elastic modulus of wheels	206 GPa
Fixed wheelbase	2.5 m
Distance between bogie pivot centers	9 m
Mass of car body	52,000 kg
Pitch inertia moment of car body	$2.31 \times 10^6 \text{ kg}\cdot\text{m}^2$
Bogie mass	3,200 kg
Pitch inertia moment of bogies	$3,120 \text{ kg}\cdot\text{m}^2$
Vertical stiffness of the primary suspension	$1.87 \times 10^3 \text{ kN/m}$
Vertical damping of the primary suspension	$5 \times 10^2 \text{ kN}\cdot\text{s/m}$

high-speed EMU. The key dynamic parameters of the tested car body are listed in Table 1.

The test was carried out at the roller test rig of the State Key Laboratory of Traction Power at Southwest Jiaotong

University, China. The roller test rig and the high-speed traction carriage are shown in Fig. 1. The excitation applied to the car body is track geometric irregularity simulated as the dynamic displacement through the roller test rig (Figure 1(a)). The track irregularity can be chosen as a standard track irregularity spectrum (e.g., Chinese high-speed spectrum, German high-speed low/high disturbance spectrum, US fifth/sixth-grade spectrum). In our case, the Chinese high-speed spectrum was applied. The actuators of the roller test rig apply dynamic displacement in the vertical direction to the rolling wheels of the test rig that are running at specific speeds to simulate the rail track geometric irregularity in the experiment.

The original passive hydraulic dampers in the secondary suspension system were replaced by the MR dampers in both leading and trailing bogies, as shown in Fig. 2. One end of the dampers was connected to the car body, and the other end linked to the bogie. Totally, four MR dampers were replaced: two dampers in leading bogie and other two in trailing bogie. A photograph of the installed MR damper is shown in Fig. 3. The dynamic behavior of the MR dampers was adjusted by



FIGURE 3. MR damper installed in the secondary suspension system.



FIGURE 5. Data acquisition system.



FIGURE 4. Electric current controller.



FIGURE 6. FBG accelerometers installed on the carriage floor in lateral and vertical directions.

using an electric current controller (Fig. 4), which wired to the MR dampers.

The power supply was 12 V, and the maximum current input was 2.0 A. The Micron Optics Model SM130 was used as a data acquisition system (Fig. 5). The data acquisition system stored the test data with a sampling frequency of 1000 Hz. FBG accelerometers, which are immune to electromagnetic interference (EMI), were installed to measure the car body vibration responses. Altogether six FBG accelerometers were installed in three locations to measure the lateral and vertical vibration responses of the car body. The installation locations of accelerometers are the front, middle, and back of the carriage floor. A photograph of the installed accelerometers on the carriage floor is shown in Fig. 6. Two displacement sensors were installed on the carriage sidewall in the lateral direction, in front and back of the carriage, to measure the rolling motion of the carriage. One end of displacement sensors was fixed to the test rig platform through a rigid stand and the other end connected to the carriage sidewall.

An exclusive MR damper was designed and manufactured according to the outcomes of previous investigation [28]. The designed MR damper was an annular-valve damper

that has a broader force range with a lower friction force. The MR dampers were designed to operate at low velocities. A maximum control force of 4 kN was achieved at velocity 1 m/s across the damper. The diameter of the designed MR damper is 79 mm, the maximum extended length is 587 mm, the minimum compressed length is 412 mm, and the stroke of the damper is 175 mm. A photograph of the tested MR dampers is shown in Fig. 7. The full-scale roller tests were conducted in which the excitation was applied to the car body through the rolling test rig as follows. First, the speed of the rolling test rig was set to the specific speed levels, i.e., 80, 120, 160, 200, 240, 280, 320, and 350 km/hr, respectively. For each speed level, the MR dampers were tuned to six current input levels, 0, 0.4, 0.8, 1.2, 1.6, and 2.0 A, which is tantamount to six trains being tested, each having a different suspension system. At each current input case, while the wheels of the rolling test rig were activated in rolling motion, the actuators of the rolling test rig, which simulate the rail track geometric irregularity, imposed dynamic displacement in the vertical direction to the rolling wheels for about 20 seconds. For each operating condition of the test, the car body's responses were collected through the



FIGURE 7. The devised MR dampers.

TABLE 2. Operating conditions in the full-scale roller test.

	Train running speed (km/hr)	Electric current input to MR dampers					
		0 A	0.4 A	0.8 A	1.2 A	1.6 A	2.0 A
	80	✓	✓	✓	✓	✓	✓
	120	✓	✓	✓	✓	✓	✓
	160	✓	✓	✓	✓	✓	✓
	200	✓	✓	✓	✓	✓	✓
	240	✓	✓	✓	✓	✓	✓
	280	✓	✓	✓	✓	✓	✓
	320	✓	✓	✓	✓	✓	✓
	350	✓	✓	✓	✓	✓	✓

sensors deployed on the tested carriage and used for ride comfort evaluation. All in all, 48 combinations of train speeds and damper properties were tested. The full-scale roller test operating conditions are presented in Table 2.

III. RIDE COMFORT INDICES

The terminology “ride comfort” is generally used to describe the degree of human comfort on a moving vehicle. In this section, different ride comfort indices are employed to quantify the vehicle’s dynamic performance under various train running speeds and current inputs to the MR dampers; the effect of the MR dampers on the ride comfort of the high-speed train is investigated through full-scale roller tests. The widely adopted ride comfort indices are mainly related to the human being’s feeling when exposed to vibration and can be calculated from the measured acceleration data during train operation. Different rules can be defined to evaluate the ride comfort of passengers on a train. In this study, the ride comfort of the high-speed train will be evaluated based on Sperling and UIC513 rules. Both methods define the ways to assess the ride comfort by synthetically evaluating vibration ingredients in a range of sensitive frequencies.

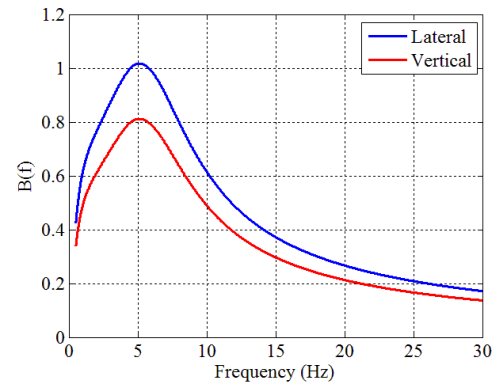


FIGURE 8. The weighting factor B(f) versus frequency.

TABLE 3. Sperling ride comfort evaluation.

Ride comfort index	Ride comfort evaluation
1	just noticeable
2	clearly noticeable
2.5	more pronounced but not unpleasant
3	strong, irregular, but still tolerable
3.25	very irregular
3.5	extremely irregular, unpleasant, annoying; prolonged exposure intolerable
4	extremely unpleasant; prolonged exposure harmful

A. SPERLING RIDE COMFORT INDEX

The Sperling index, which can quantify train ride comfort in both lateral and vertical directions respectively, is chosen as the ride comfort index, which is defined by (1) for stochastic vibration cases [24]:

$$W = \left(\int_{0.5}^{30} a^3(f) B^3(f) df \right)^{0.1} \tag{1}$$

where W is the Sperling index for ride comfort assessment. $a(f)$ is the amplitude of the spectral component of the car body acceleration corresponding to the oscillation frequency f , and $B(f)$ is the acceleration weighting factor. A smaller index value indicates a better ride experience. It is worth noting that for ride comfort evaluation, the weighting factor $B(f)$ is defined as:

$$B(f) = k \sqrt{\frac{1.911f^2 + 0.0625f^4}{(1 - 0.277f^2)^2 + (1.563f - 0.0368f^3)^2}} \tag{2}$$

where the coefficient k is decided according to vibration direction: $k = 0.588$ for vertical ride comfort and $k = 0.737$ for lateral ride comfort. Fig. 8 shows the variation of $B(f)$ versus frequency in both lateral and vertical directions, according to (2). It is seen that the dynamic response components in the frequency range of 0.5 to 10 Hz contribute dominantly to the ride comfort index. Therefore, attenuation of vibrations in this frequency range would be essential for

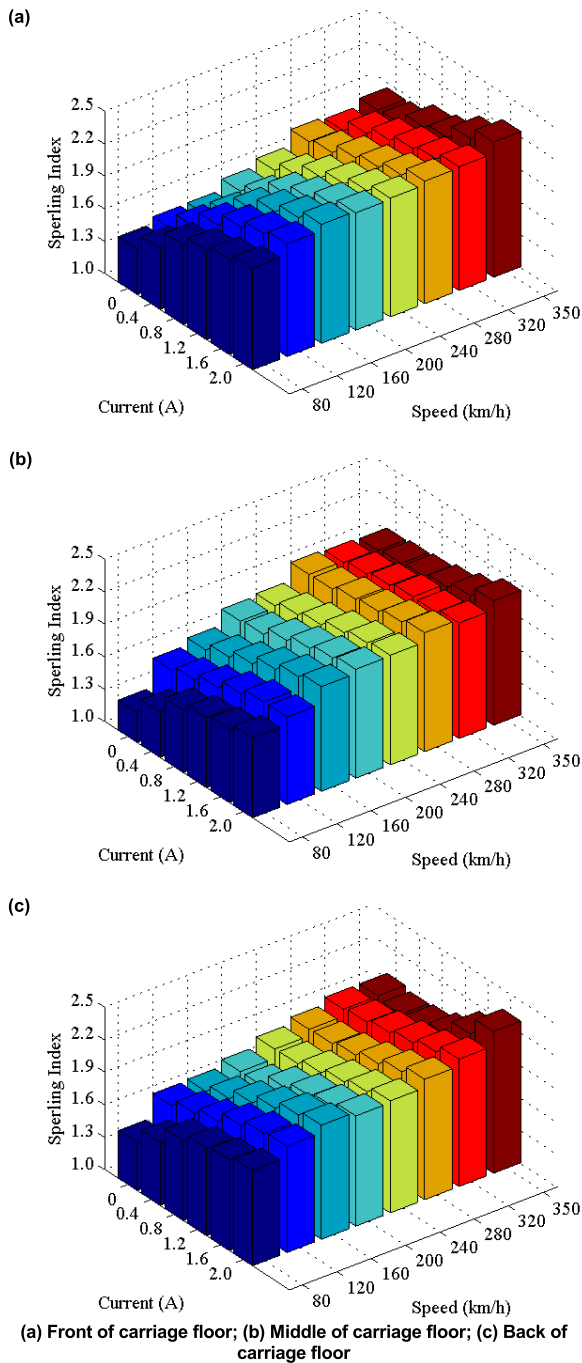


FIGURE 9. Lateral Sperling index under different test conditions.

an optimal state of the manufactured MR dampers and the suspension system. The Sperling ride comfort evaluation is presented in Table 3.

With the obtained Sperling index values, the effect of the MR dampers on ride comfort with the variation in current input to the dampers can be evaluated. Fig. 9 and Fig. 10 shows the lateral and vertical Sperling ride comfort indices, respectively, obtained under different train speeds and current inputs. According to the Sperling evaluation results, it is observed that:

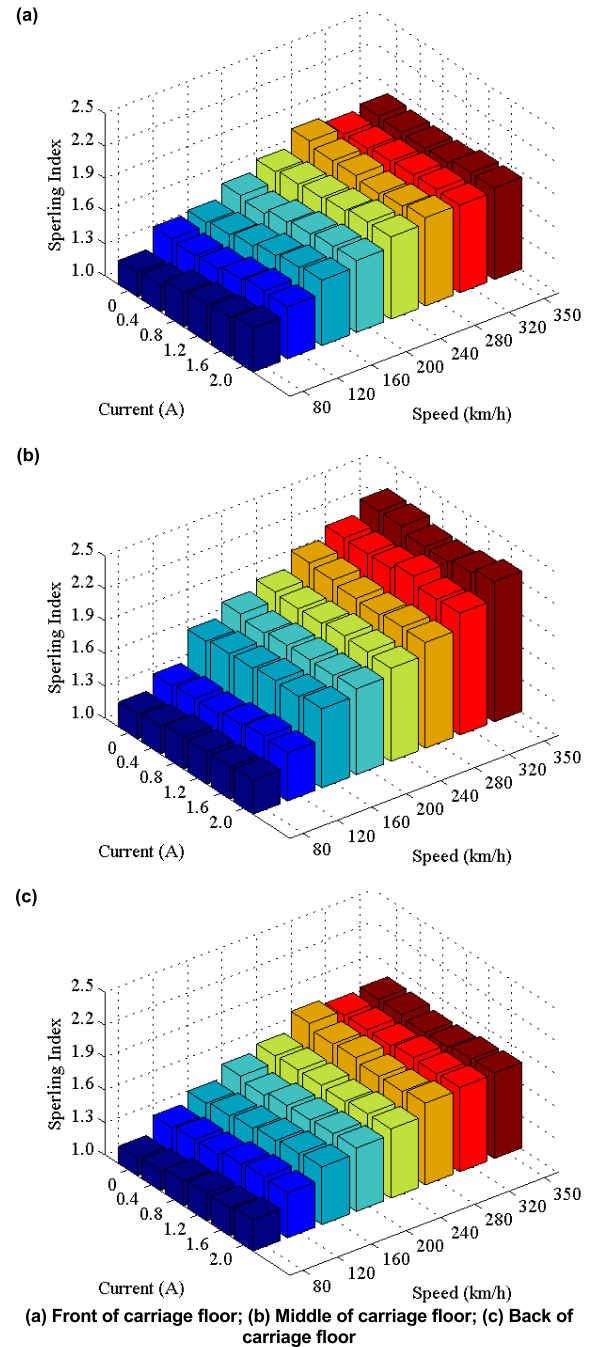


FIGURE 10. Vertical Sperling index under different test conditions.

- In both lateral and vertical directions, the car body vibration is categorized as “clearly noticeable” by passengers, but it is not unpleasant.
- Both the lateral and vertical Sperling indices increase when the train speed is increased.
- In the lateral direction, the comfort levels at different locations are almost the same.
- The current input has no significant effect on the vertical Sperling index since the MR dampers are deployed in the lateral direction and only affect the transverse motions of the vehicle.

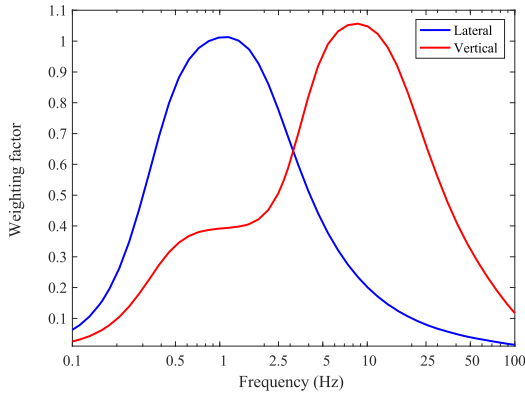


FIGURE 11. UIC513 frequency weighting curves.

TABLE 4. UIC513 ride comfort evaluation.

Ride comfort index	Ride comfort evaluation
$N < 1$	very good
$1 \leq N < 2$	good
$2 \leq N < 4$	moderate
$4 \leq N < 5$	poor
$N \geq 5$	very poor

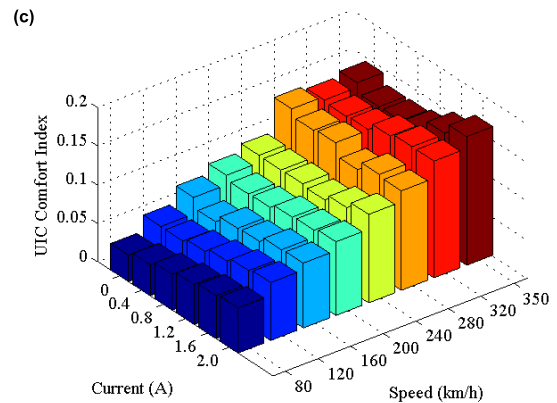
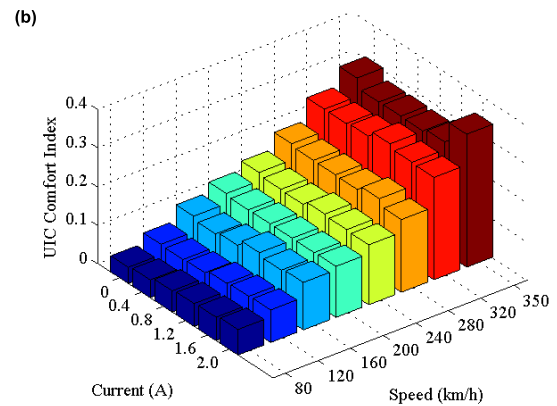
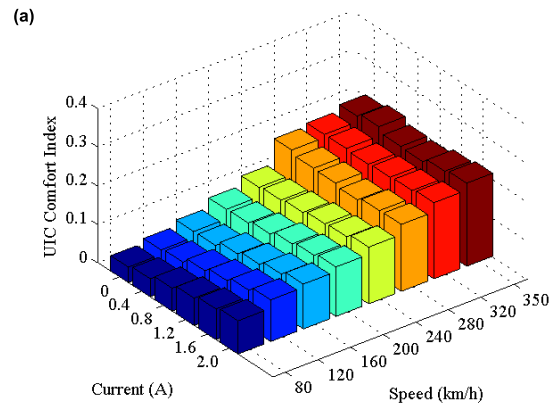
- For running speed lower than 240 km/h, the lateral Sperling index increases proportionally to the current input. However, at higher running speed (≥ 240 km/h), the lateral Sperling index remains at low values when the current input is less than 1.2 A.

B. UIC513 RIDE COMFORT INDEX

The definition of ride comfort index stipulated in UIC513 is related to the measurement of accelerations in all three directions [30]. Hence, at each measurement location, sensors should be positioned orthogonally according to the X-Y-Z reference frame, with X, Y, and Z denoting the longitudinal, lateral, and vertical directions, respectively. Further information about the configuration of the measurement points can be found in UIC513. The UIC513 provides three measurement methods and the corresponding calculation formulas for evaluating ride comfort, including two full methods for seating position and standing position, and a simplified method for seating (or standing) position [30]. The simplified method is adopted in this study. Following this method, the ride comfort index, denoted by N_{MV} , is obtained according to (3):

$$N_{MV} = 6\sqrt{(a_{XP95}^{W_d})^2 + (a_{YP95}^{W_d})^2 + (a_{ZP95}^{W_b})^2} \quad (3)$$

where $a_{XP95}^{W_d}$, $a_{YP95}^{W_d}$, and $a_{ZP95}^{W_b}$ are the weighted root mean square (RMS) values of the carriage floor accelerations in X, Y, and Z directions, respectively. The superscripts W_d and W_b denote that the frequencies are weighted in accordance with the corresponding weighting curves. The subscripts XP95, YP95, and ZP95 denote that RMS values of the



(a) Front of carriage floor; (b) Middle of carriage floor; (c) Back of carriage floor

FIGURE 12. UIC513 ride comfort index under different test conditions.

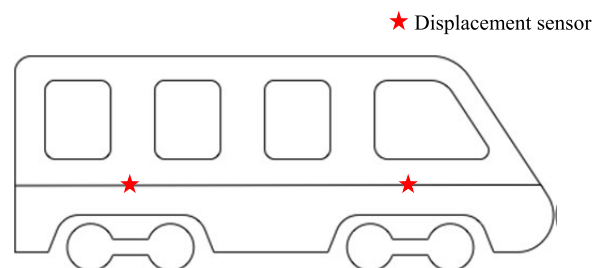


FIGURE 13. Locations of installed displacement sensors on the carriage sidewall.

accelerations regarding X, Y, and Z directions are contained in a 95% confidence interval. The frequency weighting curves W_d and W_b associated with the lateral and vertical directions are illustrated in Fig. 11.

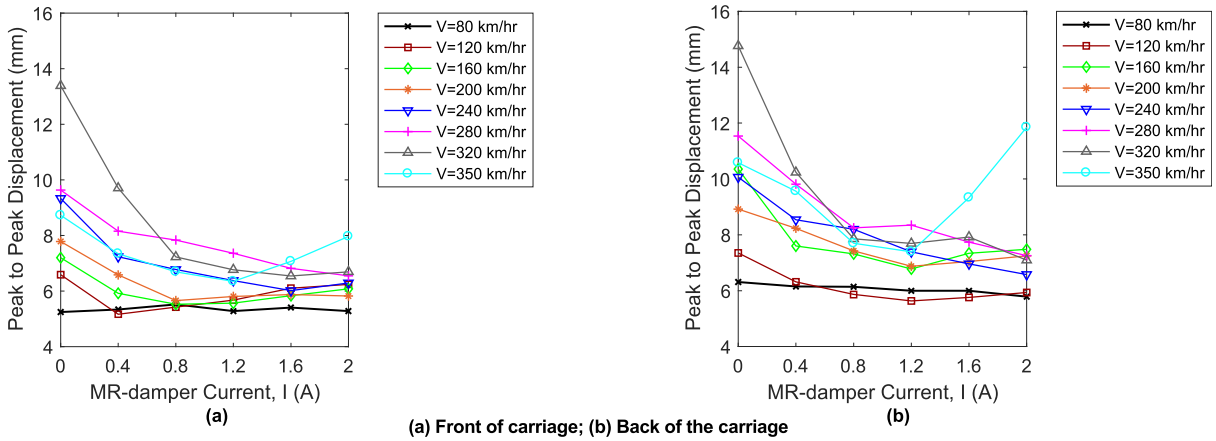


FIGURE 14. Peak to peak lateral displacement of the carriage sidewall.

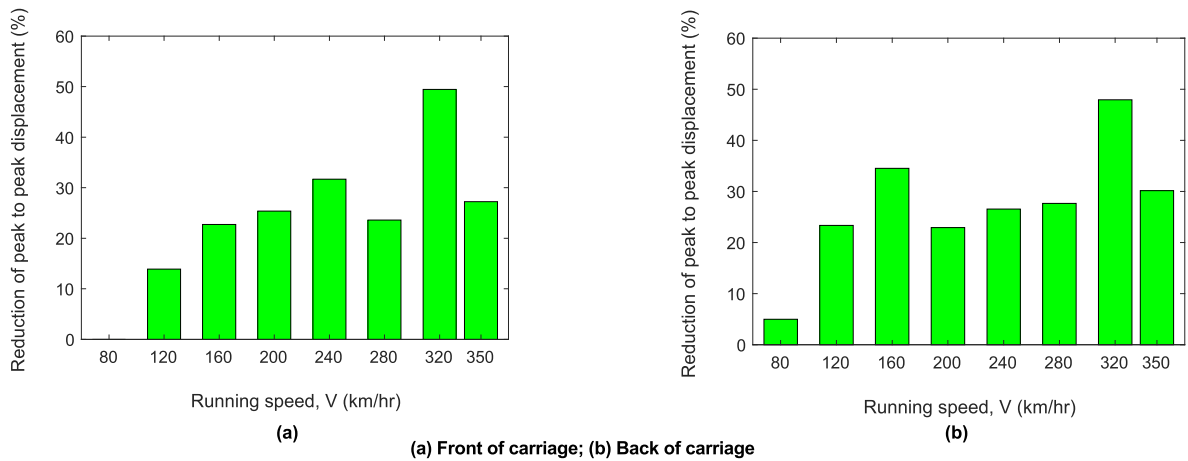


FIGURE 15. Reduction of the lateral peak to peak displacement of carriage sidewall when current input $I = 1.2$ A.

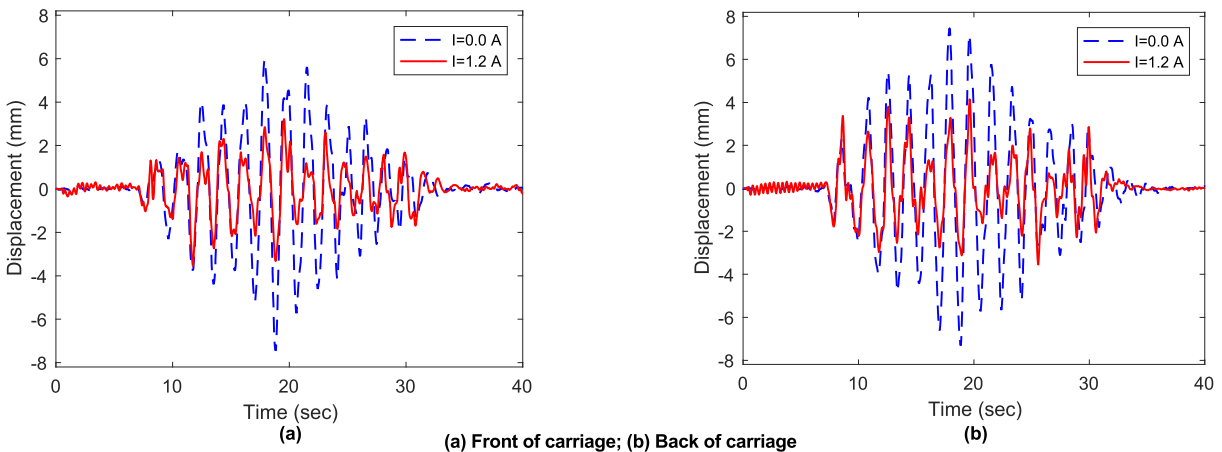


FIGURE 16. Lateral displacement time history of carriage sidewall when train speed $V = 320$ km/hr.

Five levels of ride comfort index are defined in UIC513 to describe the ride comfort perception, which are listed in Table 4. The UIC513 method is primarily used in comfort

assessment based on online monitoring, and the weighted accelerations in (3) take quantile of 95% from all the weighted acceleration values, which are calculated for sixty continuous

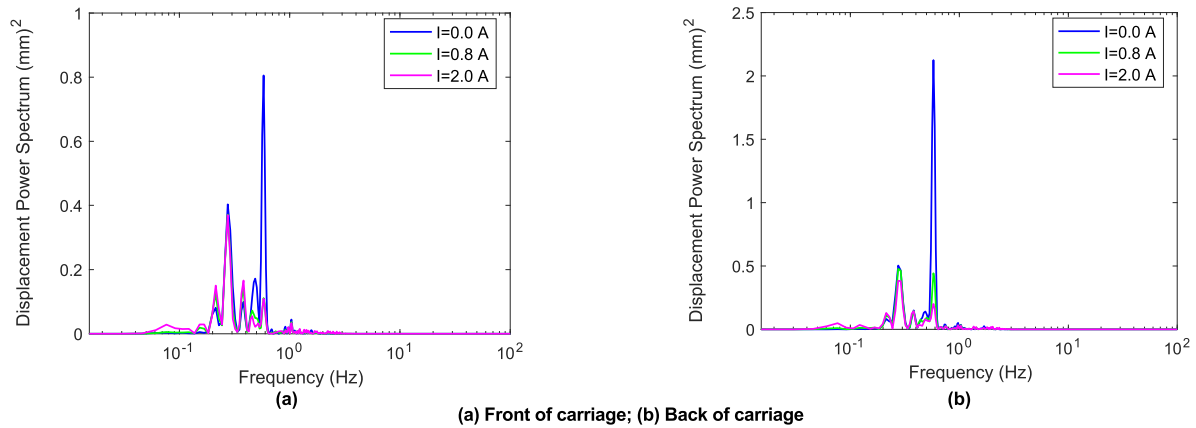


FIGURE 17. Lateral displacement power spectrum of carriage sidewall when train speed $V = 160$ km/hr.

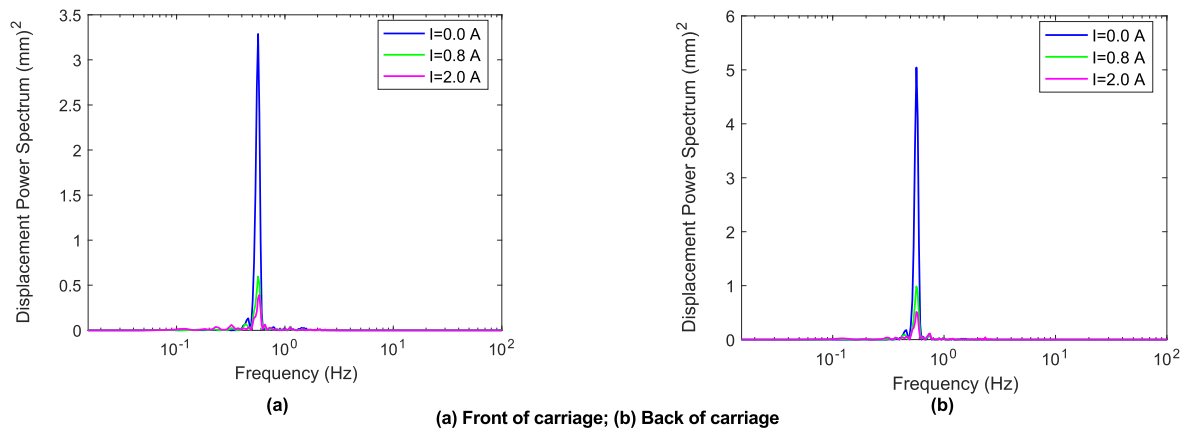


FIGURE 18. Lateral displacement power spectrum of carriage sidewall when train speed $V = 320$ km/hr.

(and not overlapping) five-second time intervals in each direction. However, since the tested car body is a single carriage and the test was conducted on a rolling test rig, the car body longitudinal vibration is not considered in this study, that is, $a_{XP95}^{W_d} = 0$.

Fig. 12 shows the UIC513 ride comfort indices obtained under different train speeds and current inputs to the dampers. According to UIC513 evaluation, it is seen that:

- A “very good comfort” level is achieved at all speed levels.
- UIC513 ride comfort indices increase with the increase of train running speed.
- Different comfort levels were observed at different locations, for instance, the ride comfort indices at the back of carriage are smaller than those at the front and middle of carriage.
- For low running speeds (≤ 120 km/h), the UIC513 ride comfort indices increase when the current input increases. However, at speeds higher than 120 km/hr, the current input has almost no significant effect on the ride comfort index.

IV. ROLLING MOTION OF CARRIAGE

In order to evaluate the ride quality, the carriage rolling motion is evaluated in this section. To this end, the absolute lateral displacement of the carriage sidewall, which corresponds to the rolling motion, is collected by two displacement sensors mounted on the sidewall at the front and back of the carriage, as illustrated in Fig. 13. The measurement was carried out in all operating conditions, as described in Table 2. As shown in Fig. 14, the peak to peak lateral displacement of the carriage sidewall is effectively reduced proportionally to current input up to 1.2 A, almost for all speed levels. However, for some speed levels (e.g., the train speed $V = 350$ km/hr), the peak to peak lateral displacement increases when the current input is higher than 1.2 A. It is evident that the rolling motion at the front of carriage is smaller than that at the back of carriage. The reduction of the peak to peak lateral displacement of carriage sidewall when current input $I = 1.2$ A and the displacement time history when train speed $V = 320$ km/hr are shown in Fig. 15 and Fig. 16, respectively. It is seen that MR dampers effectively lower the car body rolling motion.

The power spectra of the lateral displacements of carriage sidewall at different running speeds are provided in Fig. 17 and Fig. 18. As mentioned previously, rolling motion with frequencies higher than about 0.5 Hz would increase the discomfort caused by lateral oscillation. So, to improve the ride quality and passenger comfort, it is essential to mitigate rolling motion with frequencies higher than 0.5 Hz. From Fig. 17, it is seen that when the train runs at a speed of 160 km/hr, the dominant frequencies of the rolling oscillation are 0.3 Hz and 0.6 Hz. At both front and back of the carriage, the largest response occurs at the dominant frequency around 0.6 Hz, which is higher than 0.5 Hz. However, by increasing the current input to the MR dampers, the spectral peak of the lateral displacement dramatically decreases, thus mitigating the adverse effect of rolling motion. When the train running speed exceeds a certain level (≥ 280 km/hr), the dominant frequency at 0.3 Hz vanishes, and the carriage vibrates in the lateral direction just with the dominant frequency at 0.6 Hz. Fig. 18 illustrates that the MR dampers effectively reduce the spectral peak of the lateral displacement at $V = 320$ km/hr.

V. CONCLUSION

A unique and comprehensive full-scale roller test was carried out on the high-speed train model CRH3 with the intent of investigating the ride quality of the train equipped with MR dampers. An exclusive MR damper with a wider force range and lower friction force has been designed and manufactured for this purpose. The devised MR dampers were installed in the train secondary suspension system in the lateral direction, replacing the original passive hydraulic dampers. The train equipped with MR dampers ran on a roller test rig at eight running speed levels between 80 km/h to 350 km/h with track irregularity excitations being applied. In the meantime, the MR dampers were subjected to different current inputs from 0 A to 2.0 A. Altogether, 48 train operating conditions have been tested, and the car body dynamic responses were collected through a set of accelerometers and displacement sensors. To investigate the ride quality, both ride comfort and rolling motion of the carriage were evaluated. This experimental investigation proves that MR dampers effectively mitigate the carriage's rolling motion with frequencies higher than 0.5 Hz, and consequently increase the level of ride quality. It is observed that the ride comfort indices calculated from Sperling and UIC513 rules increase in general with train running speed. The current input has no significant effect on the vertical Sperling index as the MR dampers were deployed in the lateral direction, which only affect the transverse motion of the vehicle. Besides, according to the Sperling ride comfort evaluation, the car body vibration is "clearly noticeable" by passengers, but it is not unpleasant. A "very good comfort" is achieved according to the UIC513 ride comfort evaluation at all speed levels. During the tests, no train instability was observed at high speeds.

REFERENCES

- [1] W. H. Liao and D. H. Wang, "Semiactive vibration control of train suspension systems via magnetorheological dampers," *J. Intell. Mater. Syst. Struct.*, vol. 14, no. 3, pp. 161–172, Mar. 2003, doi: [10.1177/1045389X03014003004](https://doi.org/10.1177/1045389X03014003004).
- [2] R. Goodall, "Active railway suspensions: Implementation status and technological trends," *Vehicle Syst. Dyn.*, vol. 28, nos. 2–3, pp. 87–117, Aug. 1997, doi: [10.1080/00423119708969351](https://doi.org/10.1080/00423119708969351).
- [3] I. Pratt, R. M. Goodall, and A. J. Powell, "Control approaches for active lateral railway suspensions," presented at the 13th Triennial World Congr., 1996, vol. 29, no. 1, pp. 7692–7697, doi: [10.1016/S1474-6670\(17\)58928-4](https://doi.org/10.1016/S1474-6670(17)58928-4).
- [4] S. Iwnicki, *Handbook of Railway Vehicle Dynamics*, 1st ed. New York, NY, USA: Taylor & Francis, 2006, pp. 327–357.
- [5] T. X. Mei and R. M. Goodall, "Recent development in active steering of railway vehicles," *Vehicle Syst. Dyn.*, vol. 39, pp. 415–436, Aug. 2010, doi: [10.1076/vesd.39.6.415.14594](https://doi.org/10.1076/vesd.39.6.415.14594).
- [6] M. Metin and R. Guclu, "Active vibration control with comparative algorithms of half rail vehicle model under various track irregularities," *J. Vib. Control*, vol. 17, no. 10, pp. 1525–1539, Sep. 2011, doi: [10.1177/1077546310381099](https://doi.org/10.1177/1077546310381099).
- [7] R. M. Goodall, "Control for railways-active suspensions and other opportunities," presented at Proc. 19th Medit. Conf. Control Autom., 2011, pp. 639–643, doi: [10.1109/MED.2011.5983089](https://doi.org/10.1109/MED.2011.5983089).
- [8] N. D. Sims, R. Stanway, and A. R. Johnson, "Vibration control using smart fluids: A state-of-the-art review," *Shock Vib. Dig.*, vol. 31, no. 3, pp. 195–203, May 1999, doi: [10.1177/058310249903100302](https://doi.org/10.1177/058310249903100302).
- [9] V. S. Atray and P. N. Roschke, "Design, fabrication, testing, and fuzzy modeling of a large magneto-rheological damper for vibration control in a railcar," presented at the IEEE/ASME Joint Rail Conf., 2003, pp. 223–229, doi: [10.1109/RRCON.2003.1204668](https://doi.org/10.1109/RRCON.2003.1204668).
- [10] Y. K. Lau and W. H. Liao, "Design and analysis of magnetorheological dampers for train suspension," *Proc. Inst. Mech. Eng., F: J. Rail Rapid Transit*, vol. 219, no. 4, pp. 261–276, Jul. 2005, doi: [10.1243/095440905X8899](https://doi.org/10.1243/095440905X8899).
- [11] Y. K. Lau and W. H. Liao, "Pressurized magnetorheological dampers for train suspension," *Proc. SPIE*, vol. 5760, May 2005, pp. 57–68, doi: [10.1117/12.598638](https://doi.org/10.1117/12.598638).
- [12] S. Sun, H. Deng, W. Li, H. Du, Y. Q. Ni, J. Zhang, and J. Yang, "Improving the critical speeds of high-speed trains using magnetorheological technology," *Smart Mater. Struct.*, vol. 22, no. 11, Nov. 2013, Art. no. 115012, doi: [10.1088/0964-1726/22/11/115012](https://doi.org/10.1088/0964-1726/22/11/115012).
- [13] T. Jin, Z. Liu, S. Sun, Z. Ren, L. Deng, B. Yang, M. D. Christie, and W. Li, "Development and evaluation of a versatile semi-active suspension system for high-speed railway vehicles," *Mech. Syst. Signal Process.*, vol. 135, Jan. 2020, Art. no. 106338, doi: [10.1016/j.ymssp.2019.106338](https://doi.org/10.1016/j.ymssp.2019.106338).
- [14] J. D. Carlson and M. R. Jolly, "Mr fluid, foam and elastomer devices," *Mechatronics*, vol. 10, nos. 4–5, pp. 555–569, 2000, doi: [10.1016/S0957-4158\(99\)00064-1](https://doi.org/10.1016/S0957-4158(99)00064-1).
- [15] U. Dogruer, F. Gordaninejad, and C. A. Evrensel, "A new magnetorheological fluid damper for high-mobility multi-purpose wheeled vehicle (HMMWV)," *J. Intell. Mater. Syst. Struct.*, vol. 19, no. 6, pp. 641–650, Jul. 2007, doi: [10.1177/1045389X07078213](https://doi.org/10.1177/1045389X07078213).
- [16] F. Gordaninejad, X. Wang, and G. Hitchcock, "Modular high-force seismic magneto-rheological fluid damper," *J. Struct. Eng.*, vol. 136, no. 2, pp. 135–143, 2010, doi: [10.1061/\(ASCE\)0733-9445\(2010\)136:2\(135\)](https://doi.org/10.1061/(ASCE)0733-9445(2010)136:2(135)).
- [17] M. R. Jolly, J. W. Bender, and J. D. Carlson, "Properties and applications of commercial magnetorheological fluids," *J. Intell. Mater. Syst. Struct.*, vol. 10, no. 1, pp. 5–13, Jul. 2016, doi: [10.1177/1045389X9901000102](https://doi.org/10.1177/1045389X9901000102).
- [18] F. Cheli and R. Corradi, "On rail vehicle vibrations induced by track unevenness: Analysis of the excitation mechanism," *J. Sound Vib.*, vol. 330, no. 15, pp. 3744–3765, Jul. 2011, doi: [10.1016/j.jsv.2011.02.025](https://doi.org/10.1016/j.jsv.2011.02.025).
- [19] Y. K. Lau and W. H. Liao, "Design and analysis of a magnetorheological damper for train suspension," *Proc. SPIE*, vol. 5386, Jul. 2004, pp. 214–225, doi: [10.1117/12.540248](https://doi.org/10.1117/12.540248).
- [20] D. H. Wang and W. H. Liao, "Ride quality improvement ability of semi-active, active, and passive suspension systems for railway vehicles," *Proc. SPIE*, vol. 5056, Aug. 2003, pp. 201–212, doi: [10.1117/12.483462](https://doi.org/10.1117/12.483462).
- [21] G. Lauriks, J. Evans, J. Forstberg, M. Balli, and I. B. de Angoit, "UIC comfort tests," International Union of Railways, Stockholm, Sweden, Tech. Rep. VTI notat 56A-2003, Dec. 2003.
- [22] B. Kufver, R. Persson, and J. Wingren, "Certain aspects of the CEN standard for the evaluation of ride comfort for rail passengers," presented at the Int. Conf. Comput. Syst. Design Operation Railways Other Transit Syst., Southampton, U.K., vol. 2010, vol. 114, no. 1, pp. 605–614, doi: [10.2495/CR100561](https://doi.org/10.2495/CR100561).

- [23] J. Forstberg, "Ride comfort and motion sickness in tilting trains," Ph.D. dissertation, Dept. Vehicle Eng., Roy. Inst. Technol., Stockholm, Sweden, 2000.
- [24] M. Dumitriu, "Evaluation of the ride quality and ride comfort in railway vehicles based on the index W_z ," *Ann. Fac. Eng. Hunedoara-Int. J. Eng.*, vol. 13, no. 3, pp. 123–132, 2015.
- [25] G. F. Beard and M. J. Griffin, "Motion sickness caused by roll-compensated lateral acceleration: Effects of centre-of-rotation and subject demographics," *Proc. Inst. Mech. Eng., F: J. Rail Rapid Transit*, vol. 228, no. 1, pp. 16–24, Jan. 2014, doi: [10.1177/0954409712460981](https://doi.org/10.1177/0954409712460981).
- [26] H. V. Howarth and M. J. Griffin, "Effect of roll oscillation frequency on motion sickness," *Aviation, Space, Environ. Med.*, vol. 74, no. 4, pp. 326–331, Apr. 2003.
- [27] G. F. Beard and M. J. Griffin, "Discomfort caused by low-frequency lateral oscillation, roll oscillation and roll-compensated lateral oscillation," *Ergonomics*, vol. 56, no. 1, pp. 103–114, Jan. 2013, doi: [10.1080/00140139.2012.729613](https://doi.org/10.1080/00140139.2012.729613).
- [28] Y. Q. Ni, S. Q. Ye, and S. D. Song, "An experimental study on constructing MR secondary suspension for high-speed trains to improve lateral ride comfort," *Smart Struct. Syst.*, vol. 18, no. 1, pp. 53–74, Jul. 2016, doi: [10.12989/sss.2016.18.1.053](https://doi.org/10.12989/sss.2016.18.1.053).
- [29] H.-C. Kim, Y.-J. Shin, W. You, K. C. Jung, J.-S. Oh, and S.-B. Choi, "A ride quality evaluation of a semi-active railway vehicle suspension system with MR damper: Railway field tests," *Proc. Inst. Mech. Eng., F: J. Rail Rapid Transit*, vol. 231, no. 3, pp. 306–316, Mar. 2017, doi: [10.1177/0954409716629706](https://doi.org/10.1177/0954409716629706).
- [30] *Guidelines for Evaluating Passenger Comfort in Relation to Vibration in Railway Vehicles*, UIC513, International Union of Railways, Paris, France, 1994.



Y. Q. NI received the B.Eng. and M.Sc. degrees from Zhejiang University, China, in 1983 and 1986, respectively, and the Ph.D. degree from The Hong Kong Polytechnic University, Hong Kong, in 1997. He is currently a Chair Professor of smart structures and rail transit at The Hong Kong Polytechnic University. He is the Director of the National Engineering Research Center on Rail Transit Electrification and Automation (Hong Kong Branch) and the Vice President of the International Society for Structural Health Monitoring of Intelligent Infrastructure (ISHMII). His research interests include structural health monitoring, sensors and actuators, signal processing, and monitoring and control in railway engineering.



S. M. SAJJADI ALEHASHEM received the B.Eng. degree from KIAU, Karaj, Iran, in 2002, and the M.Sc. and Ph.D. degrees from Shahrood University of Technology, Shahrood, Iran, in 2005 and 2012, respectively. He is currently a Research Fellow with the Department of Civil and Environmental Engineering, The Hong Kong Polytechnic University, Hong Kong. His research interests include structural dynamics, noise and vibration control, fabricating, modeling, analysis of MR-based devices, and signal processing.



X. Z. LIU received the B.Eng. and M.Sc. degrees from Tongji University, Shanghai, China, in 2010 and 2013, respectively, and the Ph.D. degree from The Hong Kong Polytechnic University, Hong Kong, in 2018. He is currently an Assistant Professor at Shenzhen Technology University, Shenzhen, China. His research interests include railway engineering, structural dynamics, and structural health monitoring.

...